

A NOVEL DESIGN OF A SNAKE ROBOT WITH AN OPTIMIZED BATTERY DISTRIBUTION FOR EXTENDED OPERATIONAL TIME

MARWAN A. BADRAN, MD RAISUDDIN KHAN, SITI FAUZIAH TOHA*

Department of Mechatronics Engineering, Faculty of Engineering,
IIUM, Jalan Gombak, 53100, Kuala Lumpur, Malaysia

*Corresponding Author: tsfauziah@iium.edu.my

Abstract

We present a novel design of a battery distribution-based snake robot to prolong its operational time. Unlike traditional snake robot models, which utilize locomotion algorithms to reduce energy consumption, our design enhances energy capacity by integrating more batteries in a specific pattern. However, this arrangement increases the masses of the links, which affects the robot's dynamics and increases power consumption. To address this challenge, our design employs battery distribution along the snake robot's body. Furthermore, we propose a multi-objective optimization algorithm for optimal battery distribution that minimizes energy consumption while maximizing power supply capacity. Simulation results demonstrate the feasibility of the proposed design, showcasing that the power supply can be increased by 100% with only 30% increase in energy consumption.

Keywords: Energy efficiency, Lithium battery, Multi-objective optimization,
Snake robot.

1. Introduction

The field of snake robots is rapidly emerging within the realm of robotics research, with applications ranging from search and rescue missions to exploration of hazardous environments. These bio-inspired robots exhibit unique features such as agile manoeuvring and the ability to navigate through narrow passages and over rugged terrain [1]. Snake robots commonly utilize a basic undulation to perform a wave-like motion, enabling rapid crawling, climbing, and various manoeuvring tasks [2]. Exploiting such remarkable features, researchers have proposed several models of snake robots in the literature that cover a wide range of applications. Consequently, different gait models have been proposed, including planar, sidewinding and 3D gaits [3, 4].

Typically, existing snake robots are comprised of multiple rigid links, which are manipulated by servomotors to replicate the structure and locomotion gaits of real snakes [5]. Consequently, several studies have proposed a snake robot structure that utilizes soft links to achieve the flexible and continuous bending that emulates the natural movement of snakes [6, 7]. As autonomous robots, snake robots rely on rechargeable power supplies, such as Lithium-ion batteries, to facilitate their locomotion.

However, a critical aspect of autonomous snake robots is the limitation of the energy supply, as they are usually powered by a limited number of batteries. This limitation directly affects the mobility, operational time, and overall performance of the snake robot. Hence, the objective of minimizing energy consumption has mainly been achieved by developing gait algorithms for controlling the movement of the snake robot [8].

In this paper, we present a novel design for a snake robot that incorporates a distributed battery system. The primary objective of the proposed design is to extend the operational time of the snake robot by addressing the power limitations often encountered in traditional models. The proposed optimization algorithm and design are for snake robot motion on plane surfaces only. The paper is organized as follows. Section 2 provides a review of the related research work. Section 3 offers a detailed description of the proposed design, including the mathematical model and software setup. Section 4 outlines the simulation and experimental results, along with their analysis. Finally, Section 5 discusses the conclusions drawn from our findings and highlight potential future research directions.

2. Related Work

The research work in the literature has covered different aspects of snake robots. The versatility of a snake robot allows it to undertake a broad array of tasks, despite its simple structure. Consequently, extensive research has been conducted on the design and control methods employed for snake robots [9].

Recent research in evolutionary robotics [10] has demonstrated that integrating energy efficiency into robot design can lead to faster and more effective robots with diverse designs, highlighting the importance of optimized energy distribution. Another study [7] has shown that employment of plate-springed parallel elastic actuators can significantly enhance the efficiency of planar snake robots. These actuators achieve better energy efficiency compared to the traditional designs when optimizing spring stiffness using dynamic simulations.

However, the concern of this paper is the prolong the operational time of the snake robot. That objective can typically be achieved either by the mechanical design or the gait controller. It was observed that very few studies focused on the first method, such as the study by Duivon et al. [11]. The researchers proposed a design a low-cost modular snake robot controlled by elastic actuators. The design, which was built using Robot Operating System (ROS), included an eddy current damper and a battery set in each module to increase the total battery capacity, and hence, prolong the operational time.

However, including those batteries for each module will increase the power consumption due to the increased mass of the snake robot, which hasn't been addressed in the study. Furthermore, no experimental results of the proposed model were included in the study to prove its efficiency.

Similarly, a study by Bianchi et al. [12] on swimming snake robots highlighted the benefits of a bioinspired design that mimics the locomotion of anguilliform fish. The study proposed a robot with a modular design that incorporates a battery within each unit, allowing it to navigate narrow and challenging environments for extended periods. However, the study did not explore optimizing battery distribution to further prolong operational time, leaving significant potential for improvement through more effective battery distribution strategies.

In the same context, recent advancements in flexible battery design, such as the bidirectional snake-origami lithium-ion batteries proposed by Li et al. [13], have been applied to bendable robot arms, offering valuable insights for snake robots. These batteries combine rigid and soft segments to achieve high energy density and flexibility. This design could be adapted to optimize battery distribution in snake robots, enhancing energy efficiency and operational time while maintaining flexibility and minimizing mass.

Generally, most researchers have focused on controlling the gait of the snake robot to reduce energy consumption and enhance its operational time. However, some studies have proposed replacing the rigid links of the snake robot with soft links to decrease the overall mass, leading to reduced power consumption and improved energy efficiency [6]. Moreover, in other studies, a muscle-driven mechanism was employed to achieve both energy efficiency and optimal locomotion for snake robots [14].

The gait control is usually enhanced by applying Artificial Intelligence (AI) techniques such as machine learning to achieve a gait that minimizes power consumption. For example, Rebolledo et al. [15] investigated the impact of energy consumption on the behaviour and morphology of evolved robots, specifically snake-like ones. Consequently, energy consumption and speed were defined as the dual objectives for robot evolution, whereas NSGA-II (Non-dominated Sorting Genetic Algorithm II) was used for solving the multi-objective problem. The results of the study demonstrated that integrating energy efficiency into the optimization process can yield smaller robots maintaining the same speed or faster robots with the same size.

Utilizing the capabilities of machine learning, a snake robot gait design presented by Bing et al. [16] employed Reinforcement Learning (RL) to achieve an energy-efficient gait and adaptive locomotion. The RL-based method demonstrated better performance in terms of energy efficiency compared to the traditional kinematic-

based methods. Similarly, Liu and Farimani [17] applied deep reinforcement learning to develop a snake robot gait to enhance energy utilization. Compared to conventional control techniques, the proposed method achieved a considerable reduction in energy consumption and slightly improved the slithering velocity.

Typically, the utilization of snake robots for a specific task, such as navigation, requires a trade-off between locomotion speed and energy consumption, making the application of multi-objective algorithms becomes valuable in such scenarios. Singh et al. [18] combined the capabilities of reinforcement learning and fuzzy inference system to optimize an energy-efficient gait of a snake robot. The proposed multi-objective method addressed the challenge of balancing the average velocity and power consumption through a weighted-sum optimization approach. The use of a fuzzy inference system provides the advantage of accelerating learning speed by reducing the number of potential states. The proposed method achieved a faster steady-state compared to traditional approaches.

Another utilization of a multi-objective framework was introduced by Hannigan et al. [19] for controlling the gait of snake robots. The proposed method doesn't rely on predefined patterns to generate the undulation curve of the snake robot motion. Instead, the authors employed a model predictive control method to generate efficient locomotion gaits, which is adapted to the modelled environment of the snake robot as an integral aspect its dynamics. Furthermore, the study utilized the Pareto curve to describe the trade-off between achieving the desired speeds and maintaining the lowest power consumption. However, it is crucial to consider the reduction of computation time to fulfil the demands of real-time applications.

3. Description of the Proposed Design

This section describes the proposed design of the snake robot, encompassing its structure, mathematical model, and simulation setup. The primary focus of this section is to investigate the impact of battery distribution along the body of the snake robot on energy consumption. Additionally, we will present the optimization algorithm used for determining the optimal battery distribution.

Studies on snake robots by Chen et al. and Badran et al. [20, 21] have shown that the torques of the motors near the middle of the snake robot are higher than those located further away from the middle. Consequently, the energy consumption of the motors at both ends is lower. Distributing batteries along the links would disrupt this pattern of energy consumption and lead to unexpected results.

With this hypothesis, we propose a design that follows a common configuration found in the majority of snake robots, consisting of n identical links joined and actuated by $n-1$ servomotors. The main distinguishing feature of this design is that each link is equipped with a battery housing on its top, capable of holding a varying number of batteries to serve as a power source for the snake robot, as shown in Fig. 1. However, the masses of those batteries add extra load that should be considered in the calculations of energy consumption.

Ultimately, it is crucial to highlight the complexity involved in bringing the proposed design of the snake robot into a physical reality. Commonly, this implementation involves utilizing several components, including the microcontroller board, servomotor drive, connecting wires, passive wheels, and more. Furthermore, the incorporation of multiple batteries, especially in parallel

form, requires implementing a battery management system to improve energy efficiency. However, the detailed discussion of these specific details lies beyond the scope of this study.

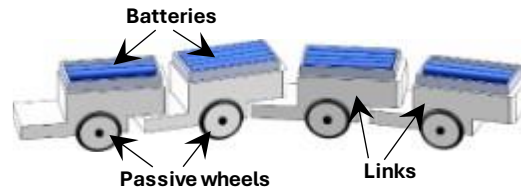


Fig. 1. A schematic 3D view of the proposed design.

3.1. Mathematical model for energy consumption

In snake robot locomotion, most of the energy is primarily consumed by the servomotors, as they draw a higher current than the electronic boards. Meanwhile, the microcontroller and the other electronic components consume a small amount of energy and, hence, will be neglected in this study. However, to obtain a comprehensive assessment, we will consider the total energy consumption of all joints in the snake robot throughout its locomotion.

To better understand the kinematic parameters involved, Fig. 2 illustrates the kinematic model of the snake robot.

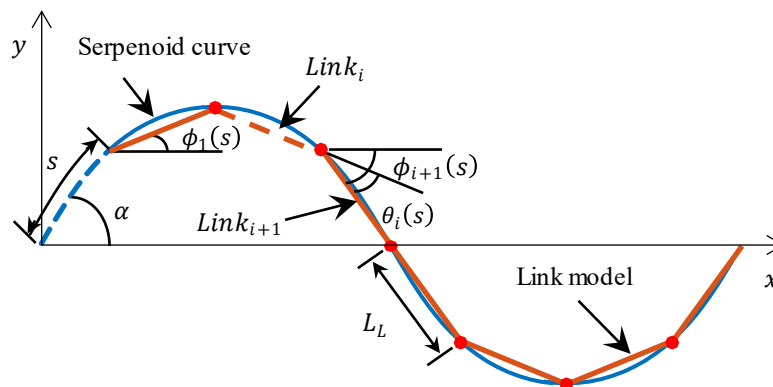


Fig. 2. A kinematic model scheme of the snake robot.

where ϕ_i represents the absolute angle between each link and the axis along the snake robot's body, and θ_i denotes the relative angle between consecutive links. These angles play a crucial role in calculating the energy consumption across the snake robot's joints, while their relation can be determined as follows:

$$\phi(i) = \phi(1) + \sum_{j=1}^{i-1} \theta_j \quad (1)$$

The following calculations are based on the proposed model by Chen et al. [20] and its modified version in our previous study [21], where the detailed derivation of the mathematical model is illustrated.

Firstly, the total energy consumption by a snake robot when traveling a specific distance can be calculated as follows:

$$E_T = \sum_{i=1}^n \int_0^T |\tau_i \dot{\theta}_i| dt \quad (2)$$

where T is the total travelling time, $\dot{\theta}$ is the angular velocity of link i , and τ_i is the torque exerted by the motor at joint i that can be calculated as follows:

$$\begin{aligned} \tau_i = I_i \ddot{\phi}_i - & \left(2 \sum_{j=i}^n m_i \ddot{x}_{jG} - 2 \sum_{j=i}^n F_{jx} - m_i \ddot{x}_{iG} + F_{ix} \right) L_L \sin \phi_i / 2 \\ & + \left(2 \sum_{j=i}^n m_i \ddot{y}_{jG} - 2 \sum_{j=i}^n F_{jy} - m_i \ddot{y}_{iG} + F_{iy} \right) L_L \cos \phi_i / 2 \end{aligned} \quad (3)$$

where $\ddot{\phi}$ is the angular acceleration, while \ddot{x} and \ddot{y} are the accelerations along x-axis and y-axis respectively.

From the previous equation, it can be noticed that the torque, and thus the energy consumption, are affected by the mass variation, as it will be apparent in the following equations.

The first affected variable is the moment of inertia of link i , which is calculated as follows:

$$I_i = \frac{1}{12} \left((m_L L_L^2)_i + (m_B L_B^2)_i \right) \quad (4)$$

where, m_L and L_L are the mass and the length of link i , while m_B and L_B are the mass and the length of the attached batteries to the same link. However, it should be noted that the centre of mass of the attached battery(ies) is assumed to be over the centre of mass of the link itself.

Secondly, the tangential (F_T) and lateral (F_N) friction forces are also mass-dependent and can be calculated as follows:

$$F_T = -\mu_T * \text{sign}(v_T) * m_i * g \quad (5)$$

$$F_N = -\mu_N * \text{sign}(v_N) * m_i * g \quad (6)$$

where μ_T and μ_N are the tangential and lateral coefficients of friction respectively, while v_T and v_N are the tangential and lateral velocities. Considering that m_i is the total mass of link i , it can be defined as follows:

$$m_i = m_{Li} + m_{Bi} \quad (7)$$

where m_{Li} is the mass of link i and m_{Bi} is the mass of batteries attached to link i . Thus, the mass of the attached batteries is included in the mass of the link.

Finally, the above equations can be employed in the optimization algorithm, where the masses of the links are varied to achieve the optimal battery distribution for efficient energy consumption. The optimization procedure is further detailed in the upcoming subsection.

3.2. Optimization of battery distribution

This section illustrates the optimization process of the proposed design of snake robot, focusing on battery distribution, as described in Section 3. The implementation and simulation of the proposed design were carried out using the MATLAB platform. For research purposes, the snake robot in this study comprises 8 links, and a set of batteries distributed in a specific pattern. Consequently, the battery distribution (D_B) is defined as a row vector of integer numbers as follows:

$$D_B = \{n_1, n_2, n_3, n_4, n_5, n_6, n_7, n_8\} \quad (8)$$

where $0 \leq n_i \leq 4$, for $i = 1, 2, \dots, 8$.

Similarly, the links' masses (m_L) are represented as a set of real numbers as follows:

$$m_L = \{m_1, m_2, m_3, m_4, m_5, m_6, m_7, m_8\} \quad (9)$$

where m_i is the mass of link i , for $i = 1, 2, \dots, 8$.

Finally, the resultant vector (m_T) represents the total masses of the links and can be expressed as follows:

$$m_T = (D_B \odot m_B) + m_L \quad (10)$$

where \odot denotes element-wise multiplication, while m_B is a scalar value that represents the mass of a single battery.

3.2.1. Multi-objective optimization

In this research, our primary aim is to prolong the operational time of the snake robot. To achieve this goal, we have two main objectives: the first is to increase the capacity of the power supply by employing a greater number of batteries. However, increasing the number of batteries also results in additional power demands due to an increase in mass. Therefore, we need to optimize the distribution of batteries along the body of the snake robot to achieve our second objective, which is minimizing the total energy consumption.

To address these objectives and strike a suitable trade-off, we applied a Multi-Objective Optimization (MOO) algorithm as proposed in our previous study [22]. The optimization process considers various parameters, including number of batteries, battery mass, link mass, and energy consumption. The procedure of the Multi-Objective Optimization Algorithm is provided in the following pseudocode, while the overall process can be found in Fig. 3.

Pseudocode for Multi-Objective Optimization Algorithm

```
// Step 1: Define Objective Functions
 $f_1 = \max(B)$ 
 $f_2 = \min(E)$ 

// Step 2: Define Constraints
 $C = \text{sum}(B_i) \geq 8$ , for  $i = 1$  to  $8$  // to ensure a sufficient number of batteries

// Step 3: Initialize Parameters
 $n = 8$  // number of links
 $B_{\max} = 4$  // per link
 $m_B = 30$  g // battery mass
```

```

 $M_L = 100$  g // link mass
 $D_T = 3$  m // travelling distance
 $D_B = [1\ 2\ 2\ 3\ 3\ 2\ 2\ 1]$  // battery distribution
 $C_{all} = B_{max}^n$  // calculate combinations

// Step 4: Optimization Process
while not optimal_distribution_found do
  for each  $D_B$  in  $C_{all}$  do
     $E = \text{calculate\_energy\_consumption}(D_B)$  // call fitness function

// Step 5: Evaluate Objective Functions
 $F_1 = \text{evaluate}(f_1)$ 
 $F_2 = \text{evaluate}(f_2)$ 

// Step 6: Check Optimality
if ( $F_1$  is maximized and  $F_2$  is minimized) and  $C$  is satisfied then
  optimal_distribution_found = true
  break
end if
end for
adjust( $D_B$ ) // adjust battery distribution
end while

// Step 7: Output Optimal Solution
output optimal_battery_distribution

```

The first step is to define our objective functions: the first one is to maximize the number of employed batteries, which is indicated as f_1 , while the second one is to minimize energy consumption, indicated as f_2 . Hence, the objective functions can be expressed as follows:

$$f_1 = \max(B) \quad (11)$$

$$f_2 = \min(E) \quad (12)$$

where B and E are the number of batteries and total energy consumption respectively.

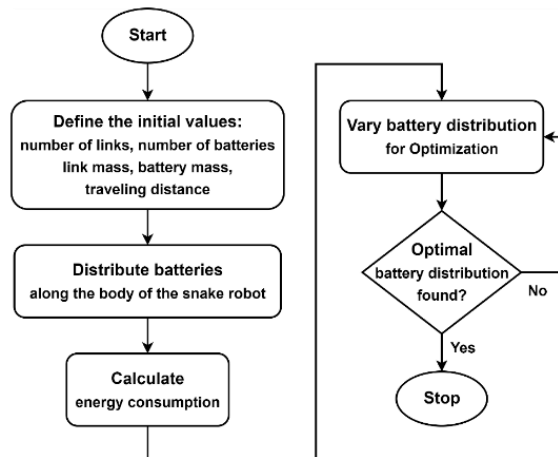


Fig. 3. Flowchart of the optimization process.

On the other hand, constraints need to be defined for the optimization process to address the limitations of the snake robot's parameters. In this study, we consider two constraints C_1 and C_2 . The first constraint ensures that the total number of batteries is at least 8, providing sufficient energy for multiple servomotors. The second constraint limits the maximum number of batteries per link to 4 to prevent overloading. Mathematically, these constraints can be expressed as follows:

$$C_1: B \geq 8 \quad (13)$$

$$C_2: b_i \leq 4, i = 1, 2, \dots, 8 \quad (14)$$

where B is the total number of batteries, and b_i is the number of batteries placed on a specific link i .

By referring to our previous study [21], the total energy consumption of a snake robot journey is mainly affected by the initial acceleration and the winding angle. However, the main concern of this paper is about the effect of mass variation on energy consumption based on battery distribution. Therefore, the initial acceleration and the winding angle will remain fixed, while the links' masses will be varied by varying the number of batteries in each link. This type of arrangement leads to a total number of different combinations of battery distribution that can be calculated as follows:

$$C_{total} = B^n \quad (15)$$

Here, B is the number of batteries, while n is the number links. For example, a snake robot of eight links equipped with a maximum of four batteries per link yields 390625 possible combinations of battery arrangement. Such a considerable number of combinations demands an optimization algorithm to efficiently reduce the number of simulations and aid in finding the optimal battery arrangement.

3.2.2. Simulation setup

In this study, we encounter two conflicting objectives: the first one is to maximize the number of employed batteries, while the second is to minimize energy consumption. To address this conflict, we utilized the *gamultiobj* function in MATLAB, which is based on the NSGA-II algorithm. This powerful multi-objective optimization algorithm was applied to the snake robot, where the energy consumption served as the fitness function. A description of the parameters utilized in the optimization process is provided in Table 1.

Table 1. Parameters of optimization algorithm.

| Parameter | Value |
|---------------------------------------|----------------------|
| Length of the link | 0.1 m |
| Mass of the link | 0.1 kg |
| Number of links | 8 |
| Length of the battery | 0.05 m |
| Mass of the battery | 0.03 kg |
| Number of batteries for a single link | 0 to 4 |
| Traveling distance | 3 m |
| Winding angle | 30° |
| Initial acceleration | 1.5 m/s ² |

The simulation process of snake robot locomotion with different battery distributions was carried out in two phases. In the first stage, the goal was to

examine the effect of different battery distributions on the total energy consumption when the snake robot travels a specific distance. To achieve this, we tested the proposed design based on selected patterns of battery distribution for assessment purposes. These patterns encompassed various arrangements, such as increasing the number of batteries and changing the order of the same number of batteries.

The second phase involved the implementation of multi-objective optimization to determine the optimal battery distribution that guarantees sufficient power supply, while keeping power consumption as minimal as possible. The simulation results are presented in the next section.

4. Results and Discussion

This section presents the simulation results that demonstrate the effect of different battery distributions on the energy consumption of an eight-link snake robot when traveling a 3-meter distance. Firstly, we tested the proposed design using selected patterns of battery distribution for evaluation purposes. These patterns included different arrangements, such as increasing the number of batteries or distributing the same number of batteries with different orders as illustrated in Fig. 4.

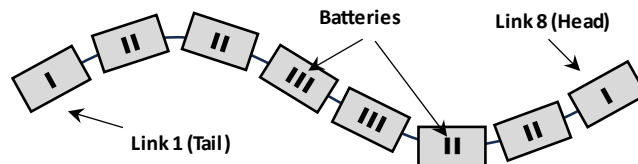


Fig. 4. Battery distribution along the snake robot's body.

The simulation results shown in Table 2 are sorted in ascending order based on energy consumption. It should be noted that the numbers in the column headers represent the links of the snake robot, while the vertical bars represent the number of batteries attached to the respective link. For instance, the symbol (II) indicates 2 batteries, whereas the symbol (III) denotes 3 batteries, and so on.

Table 2. Effect of battery distribution on energy consumption.

| Pattern No | Battery distribution along the eight links (tail to head) | | | | | | | | Energy consumption (J) | | | |
|------------|---|-----|-----|-----|-----|-----|-----|-----|------------------------|-------|-------|-------|
| | 1 | 2 | 3 | 4 | 5 | 6 | 7 | 8 | Battery mass | | | |
| | | | | | | | | | 20 g | 30 g | 50 g | 60 g |
| p_1 | I | I | I | I | I | I | I | I | 4.36 | 4.71 | 5.42 | 5.77 |
| p_2 | II | II | II | II | II | II | II | II | 5.06 | 5.77 | 7.18 | 7.88 |
| p_3 | III | III | III | III | III | III | III | III | 5.77 | 6.82 | 8.94 | 10.00 |
| p_4 | — | — | II | II | II | II | — | — | 4.25 | 4.58 | 5.57 | 6.19 |
| p_5 | — | II | II | — | — | II | II | — | 6.09 | 7.88 | 12.26 | 14.88 |
| p_6 | III | III | II | I | I | II | III | III | 5.88 | 7.03 | 9.34 | 10.51 |
| p_7 | II | II | III | III | III | III | II | II | 5.32 | 6.16 | 7.85 | 8.69 |
| p_8 | — | III | III | III | III | III | III | — | 7.58 | 11.01 | 21.12 | 27.51 |
| p_9 | II | III | III | III | III | III | II | II | 5.70 | 6.87 | 9.31 | 10.57 |

Based on the results in Table 2, it is evident that increasing the number of batteries in each link leads to higher energy consumption as observed in the first three rows. In these patterns, the number of attached batteries, and thus the

mass, was first doubled and then trebled, resulting in an almost linear increase in energy consumption.

However, it is worth noting that patterns p_1 , p_4 , and p_5 have the same number of batteries (a total of 8 batteries), yet they lead to different values of energy consumption. The same observation applies to patterns p_6 , p_7 , and p_8 , where a total of 20 batteries are distributed in different patterns.

Additionally, despite increasing the number of batteries in pattern p_9 (22 batteries), the energy consumption was reduced by approximately 38% compared to pattern p_8 (20 batteries), when using batteries with a mass of 30 g each. This reduction became more significant as the battery mass increased, demonstrating that the optimized distribution in pattern p_9 led to improved efficiency even with a higher total battery count.

However, it is crucial that the mass of the batteries remains within the limits of the servomotor's capability. Overall, the general trend of energy consumption remains consistent across different battery masses, as shown in Fig. 5, indicating that while the distribution pattern significantly impacts efficiency, the battery mass itself does not alter the fundamental trend of energy consumption.

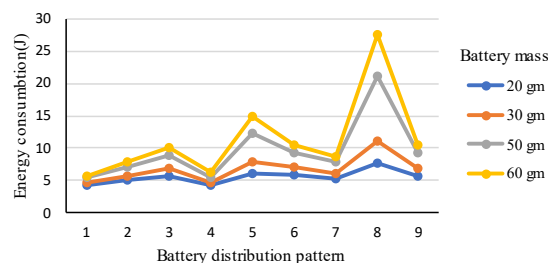


Fig. 5. Impact of battery distribution on energy consumption using different battery masses.

Further simulations were conducted to assess the impact on energy consumption when using the same total number of batteries. Results of a total of 8 batteries distributed in pairs are presented in Table 3, while results for a total of 20 batteries, symmetrically distributed, are presented in Table 4.

Table 3 displays the results obtained using four pairs of batteries distributed along the eight links. Meanwhile, the results of using 1 to 4 symmetrically distributed batteries are shown in Table 4. The simulation included all possible combinations of battery distribution; however, only a few results are presented here, which are sufficient to demonstrate the trend of the effect of battery distribution on energy consumption.

It is noted from the results in Table 3 that the concentration of batteries at the first half of the snake robot (next to the tail) in addition to the last link, tends to decrease power consumption, as seen in rows 1 to 3. Meanwhile, it is also noted that battery concentration on the second half of the snake robot (next to the head) demonstrates the highest values of energy consumption, as seen in the last row of Table 3. However, even a slight shift of the battery distribution may lead to a noticeable increase in energy consumption as seen in rows 2 and 69.

Table 3. Effect of distributing a similar number of batteries on energy consumption.

| Pattern No | Battery distribution along the eight links (tail to head) | | | | | | | | Energy cons. (J) |
|------------|---|----|----|----|----|----|----|----|------------------|
| | 1 | 2 | 3 | 4 | 5 | 6 | 7 | 8 | |
| p_1 | II | II | — | II | — | — | — | II | 2.56 |
| p_2 | II | II | II | — | — | — | — | II | 2.70 |
| p_3 | II | II | — | — | II | — | — | II | 2.80 |
| p_4 | II | — | II | II | — | — | — | II | 2.82 |
| p_5 | — | — | II | II | II | II | — | — | 2.92 |
| : | : | : | : | : | : | : | : | : | : |
| p_{60} | II | II | II | II | — | — | — | — | 6.17 |
| p_{61} | II | II | II | — | II | — | — | — | 6.23 |
| : | : | : | : | : | : | : | : | : | : |
| p_{65} | II | II | II | — | — | II | — | — | 6.65 |
| p_{66} | II | II | — | — | — | II | II | — | 6.70 |
| p_{67} | — | — | — | II | II | II | — | II | 6.78 |
| p_{68} | II | II | II | — | — | — | II | — | 6.89 |
| p_{69} | — | — | — | II | — | II | II | II | 6.95 |
| p_{70} | — | — | — | — | II | II | II | II | 7.84 |

Table 4. Effect of distributing a variant number of batteries on energy consumption.

| Pattern No | Battery distribution along the eight links (tail to head) | | | | | | | | Energy cons. (J) |
|------------|---|------|------|------|------|------|------|------|------------------|
| | 1 | 2 | 3 | 4 | 5 | 6 | 7 | 8 | |
| p_1 | I | II | III | IIII | IIII | IIII | II | I | 3.87 |
| p_2 | IIII | IIII | I | II | II | I | IIII | IIII | 4.17 |
| p_3 | IIII | IIII | II | I | I | II | IIII | IIII | 4.24 |
| p_4 | IIII | II | IIII | I | I | IIII | II | IIII | 4.25 |
| p_5 | IIII | IIII | I | II | II | I | IIII | IIII | 4.26 |
| p_6 | I | IIII | II | IIII | IIII | II | IIII | I | 4.28 |
| : | : | : | : | : | : | : | : | : | : |
| p_{17} | I | II | IIII | IIII | IIII | IIII | II | I | 4.34 |
| p_{18} | IIII | II | I | IIII | IIII | I | II | IIII | 4.51 |
| p_{19} | IIII | I | IIII | II | II | IIII | I | IIII | 4.65 |
| p_{20} | IIII | IIII | II | I | I | II | IIII | IIII | 4.71 |
| p_{21} | IIII | I | II | IIII | IIII | II | I | IIII | 4.89 |
| p_{22} | I | IIII | IIII | II | II | IIII | IIII | I | 5.35 |
| p_{23} | I | IIII | II | IIII | IIII | II | IIII | I | 5.39 |
| p_{24} | I | IIII | IIII | II | II | IIII | IIII | I | 5.93 |

On the other hand, the analysis of Table 4 shows that energy consumption is lowest with a symmetrical battery distribution centred around the middle of the snake robot, as seen in p_1 (3.87 J). Concentrating batteries heavily in the middle or at the ends generally increases energy consumption, with patterns like p_{22} to p_{24} showing higher values. Overall, a balanced, moderate distribution of batteries is most effective for minimizing energy consumption.

For further assessment, the proposed design was tested using the same battery distribution across different conditions. In the first test, initial acceleration (acc)

was fixed, while the winding angle (α) varied. In the second test, the winding angle was fixed, while the initial acceleration varied as follows:

- Case 1: $\alpha = 30^\circ$, $acc = 1.5 \text{ m/s}^2$
- Case 2: $\alpha = 45^\circ$, $acc = 1.5 \text{ m/s}^2$
- Case 3: $\alpha = 30^\circ$, $acc = 1.2 \text{ m/s}^2$

The results of these tests are presented in Table 5. The purpose of this assessment is to explore the impact of battery distribution on energy consumption when varying parameters such as winding angle and initial acceleration (which influences the average speed). The test encompassed all possible combinations of 4 pairs of batteries across the eight links of the snake robot. However, due to space constraints, only selected results are presented here. Nevertheless, the displayed results are sufficient to demonstrate the overall tendency.

Table 5. Effect of battery distribution on energy consumption using different winding angles and average speeds.

| Pattern No | Battery distribution along the eight links (tail to head) | | | | | | | | Energy consumption (J) | | |
|------------|---|----|----|----|----|----|----|----|------------------------|--------------|-------------|
| | 1 | 2 | 3 | 4 | 5 | 6 | 7 | 8 | Case 1 | Case 2 | Case 3 |
| p_1 | II | II | – | II | – | – | – | II | 2.56 | 5.99 | 2.27 |
| p_2 | II | II | II | – | – | – | – | II | 2.70 | 6.37 | 2.44 |
| p_3 | II | II | – | – | II | – | – | II | 2.80 | 6.46 | 2.41 |
| p_4 | II | – | II | II | – | – | – | II | 2.82 | 5.77 | 2.53 |
| p_5 | – | – | II | II | II | II | – | – | 2.92 | 6.38 | 2.41 |
| p_6 | II | – | II | – | II | – | – | II | 3.06 | 6.23 | 2.78 |
| : | : | : | : | : | : | : | : | : | : | : | : |
| p_{62} | II | II | – | II | – | – | II | – | 6.25 | 12.29 | 5.27 |
| p_{63} | II | II | – | – | II | – | II | – | 6.28 | 12.59 | 5.33 |
| p_{64} | – | – | – | II | II | – | II | II | 6.55 | 10.45 | 6.08 |
| p_{65} | II | II | II | – | – | II | – | – | 6.65 | 13.21 | 5.74 |
| p_{66} | II | II | – | – | – | II | II | – | 6.70 | 13.44 | 5.75 |
| p_{67} | – | – | – | II | II | II | – | II | 6.78 | 10.59 | 6.39 |
| p_{68} | II | II | II | – | – | – | II | – | 6.89 | 13.55 | 5.87 |
| p_{69} | – | – | – | II | – | II | II | II | 6.95 | 11.09 | 6.40 |
| p_{70} | – | – | – | – | II | II | II | II | 7.84 | 12.19 | 7.31 |

Results shown in Table 5 were sorted in ascending order based on Case 1 for comparison purposes. It can be observed that the lowest energy consumption is achieved using pattern p_1 in both Case 1 and Case 3. Similarly, pattern p_{70} yielded the highest energy consumption in both cases. The other patterns have a nearly similar effect on energy consumption, indicating that changing the average speed did not significantly alter the general impact of battery distribution for the same winding angle.

On the other hand, when the winding angle increases from 30° to 45° while maintaining the same average speed (Case 1 vs. Case 2), energy consumption generally rises across all battery distributions. The extent of this increase varies, showing that the impact of battery distribution on energy consumption is influenced by changes in the winding angle. Some distributions lead to a more pronounced

increase in energy consumption than others, suggesting that certain distributions are less optimal at higher winding angles.

However, while the effect of winding angle and average speed on energy consumption has been extensively explored in our previous work [21], this paper focuses specifically on optimizing battery distribution for efficient energy consumption. The findings underscore the critical importance of optimizing battery distribution patterns to achieve energy efficiency across different operating conditions. By carefully selecting and optimizing these patterns, it is possible to minimize energy usage and extend the operational time of the snake robot.

The results shown previously in this paper discussed the effect of preselected patterns of battery distribution on energy consumption. However, the process of finding the optimal battery distribution is a tricky task, especially when the number of batteries is undefined. Furthermore, the simulation result of the multi-objective optimization is shown in Fig. 6 as a set of points forming a Pareto optimality curve. The graph effectively visualizes the trade-offs between battery distribution patterns and energy consumption.

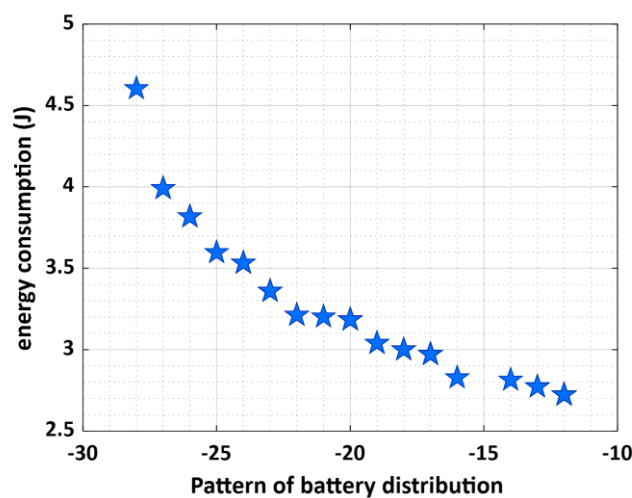


Fig. 6. Pareto optimality curve of battery distribution patterns vs. energy consumption.

It should be noted that the integer numbers along the x-axis in Fig. 6 indicate the summation of batteries for a specific pattern, while the negative sign is employed for optimization purposes. Each point on the curve in Fig. 6 depicts an optimal solution that strikes a different balance between the two objectives. The Pareto optimality curve provides valuable insights into the trade-offs between conflicting objectives, including solutions that cannot be improved in one objective without sacrificing the other. However, there are some techniques, such as the weighted sum method, that help in selecting the best solution, which is beyond the scope of this study.

To conduct further analysis, the battery distribution patterns were extracted from the results shown in the Pareto optimality curve and subsequently transferred to Table 6.

Table 6. Solutions obtained by Pareto optimality curve.

| Pattern No | Battery distribution along the eight links (tail to head) | | | | | | | | Total batteries | Energy cons. (J) |
|------------|---|-----|-----|-----|-----|-----|-----|-----|-----------------|------------------|
| | 1 | 2 | 3 | 4 | 5 | 6 | 7 | 8 | | |
| p_1 | II | II | II | II | I | I | – | II | 12 | 2.72 |
| p_2 | II | II | II | II | II | I | – | II | 13 | 2.77 |
| p_3 | III | III | II | II | I | – | – | III | 14 | 2.81 |
| p_4 | III | III | II | III | II | – | – | III | 16 | 2.83 |
| p_5 | III | III | II | III | II | I | – | III | 17 | 2.97 |
| p_6 | III | III | III | III | II | I | – | III | 18 | 3.00 |
| p_7 | III | III | III | III | III | I | – | III | 19 | 3.04 |
| p_8 | III | III | III | III | III | II | – | III | 20 | 3.18 |
| p_9 | III | III | III | III | II | I | – | III | 21 | 3.20 |
| p_{10} | III | III | III | III | III | I | – | III | 22 | 3.21 |
| p_{11} | III | III | III | III | III | II | – | III | 23 | 3.36 |
| p_{12} | III | III | III | III | III | III | – | III | 24 | 3.53 |
| p_{13} | III | III | III | III | III | II | I | III | 25 | 3.60 |
| p_{14} | III | III | III | III | III | II | II | III | 26 | 3.82 |
| p_{15} | III | III | III | III | III | III | II | III | 27 | 3.99 |
| p_{16} | III | III | III | III | III | III | III | III | 28 | 4.60 |

The solutions presented in Table 6 utilize various numbers of batteries and diverse patterns. However, the majority of these solutions suggest no batteries on link 6 and a minimal number for link 6. Essentially, all the solutions in Table 6 are acceptable; however, some solutions offer better results. For instance, when comparing patterns p_1 (with 12 batteries) and p_{12} (with 24 batteries), we notice that the number of batteries was twice that of pattern p_1 , while the energy consumption increased by only 30%. In simple terms, by utilizing this arrangement, we can double the capacity of the power supply at the cost of only 30% of extra energy consumption. Consequently, the battery distribution of pattern p_{12} demonstrates more efficient utilization of energy compared to pattern p_1 .

5. Conclusion

In this paper, a novel design for a snake robot with a battery distribution along its body is proposed. The main contribution of this work is introducing an innovative approach to leverage the snake body in increasing the power supply capacity by adding more batteries, thereby significantly prolonging the operational time of the snake robot. The simulation results demonstrate that the proposed design effectively improves the efficiency of the snake robot by optimizing the battery distribution along its body. Notably, different distributions of the same total number of batteries may reduce energy consumption by approximately 38%. Moreover, the simulations consistently revealed that battery concentration near the middle of the snake robot consumes less energy compared to concentration near the ends.

Furthermore, a multi-objective optimization based on the NSGA-II algorithm was applied to derive the optimal battery distribution, resulting in a Pareto optimality curve that accounts for the trade-offs between the number of batteries and energy consumption. Notably, we observed that certain arrangements of battery distribution can effectively double the capacity of the power supply with just an additional 30% of energy consumption.

A potential limitation of the design is finding batteries of the appropriate size that fit the snake robot and are optimally placed without affecting its balance. Addressing this issue will involve exploring suitable battery sizes and optimizing their placement. Looking ahead, potential future work may focus on optimizing the link size and number of links to achieve a snake robot design that extends operational time by minimizing total energy consumption. Additionally, machine learning techniques hold promise for modelling the snake robot based on battery distribution, presenting exciting possibilities for further advancements in this field.

Future research could explore optimizing battery distribution in various scenarios and integrating advanced control systems. Practical applications include search and rescue, environmental monitoring, and industrial inspections.

Nomenclatures

| | |
|-------------------|--|
| acc | Initial acceleration, m/s^2 |
| B | Number of batteries |
| C_{total} | Total number of different combinations of battery distribution |
| D_B | Row vector of battery distribution |
| E_T | Total energy consumption, J |
| F_n | Lateral friction force, N |
| F_t | Tangential friction force, N |
| g | Gravitational acceleration, m/s^2 |
| G | Centre of gravity, m |
| I | Moment of inertia, $kg.m^2$ |
| L_B | Length of battery, m |
| L_L | Length of the link, m |
| m_B | Mass of battery, kg |
| m_L | Mass of the link, kg |
| n | Number of links |
| p_1, p_2, \dots | Pattern numbers of different battery distributions |
| \ddot{x} | Acceleration along x-axis, m/s^2 |
| \ddot{y} | Acceleration along y-axis, m/s^2 |

Greek Symbols

| | |
|---------------|------------------------------------|
| α | Winding angle, deg. |
| θ | Relative angle, deg. |
| μ_N | Coefficient of lateral friction |
| μ_T | Coefficient of tangential friction |
| τ | Joint torque, N.m |
| ϕ | Absolute angle, deg. |
| $\ddot{\phi}$ | Angular acceleration, rad/s^2 |

Abbreviations

| | |
|---------|--|
| AI | Artificial Intelligence |
| MOO | Multi-Objective Optimization |
| NSGA-II | Non-dominated Sorting Genetic Algorithm II |
| RL | Reinforcement Learning |
| ROS | Robot Operating System |

References

1. Fu, Q.; Gatt, S.W.; Mitchell, T.W.; Kim, J.S.; Chirikjian, G.S.; and Li, C. (2020). Lateral oscillation and body compliance help snakes and snake robots stably traverse large, smooth obstacles. *Integrative and comparative biology*, 60(1), 171-179.
2. Martz, J.; Al-Sabban, W.; and Smith, R.N. (2020). Survey of unmanned subterranean exploration, navigation, and localisation. *IET Cyber-Systems and Robotics*, 2(1), 1-13.
3. Ariizumi, R.; and Matsuno, F. (2017). Dynamic analysis of three snake robot gaits. *IEEE Transactions on Robotics*, 33(5), 1075-1087.
4. Cao, Z.; Zhang, D.; and Zhou, M. (2021). Modelling and control of hybrid 3-D gaits of snake-like robots. *IEEE Transactions on Neural Networks and Learning Systems*, 32(10), 4603-4612.
5. Seeja, G.; Selvakumar Arockia Doss, A., and Hency, V.B. (2022). A survey on snake robot locomotion. *IEEE Access*, 10, 112100-112116.
6. Wan, Z.; Sun, Y.; Qin, Y.; Skorina, E.H.; Gasoto, R.; Luo, M.; Fu, J. and Onal, C.D. (2023). Design, analysis, and real-time simulation of a 3D soft robotic snake. *Soft Robotics*, 10(2), 258-268.
7. Kakogawa, A.; Kawabata, T.; and Ma, S. (2021). Plate-springed parallel elastic actuator for efficient snake robot movement. *IEEE/ASME Transactions on Mechatronics*, 26(6), 3051-3063.
8. Liu, J.; Tong, Y.; and Liu, J. (2021). Review of snake robots in constrained environments. *Robotics and Autonomous Systems*, 141, 103785.
9. Matsuno, F. et al. (2019). *Development of tough snake robot systems*. In Tadokoro, S. (Ed.), *Disaster robotics: Results from the ImPACT tough robotics challenge*. Springer International Publishing, 267-326.
10. Rebolledo, M.; Zeeuwe, D.; Bartz-Beielstein, T.; and Eiben, A.E. (2022). Co-optimizing for task performance and energy efficiency in evolvable robots. *Engineering Applications of Artificial Intelligence*, 113, 104968.
11. Duivon, A.; Kirsch, P.; Mauboussin, B.; Mougard, G.; Woszczyk, J.; and Sanfilippo, F. (2022). The redesigned serpens, a low-cost, highly compliant snake robot. *Robotics*, 11(2), 42.
12. Bianchi, G.; Mudiyansele, K.P.H.H.; and Cinquemani, S. (2022). Design of a swimming snake robot. *Proceedings of the Bioinspiration, Biomimetics, and Bioreplication XII*, Long Beach, United States.
13. Li, N.; Chen, H.; Yang, S.; Yang, H.; Jiao, S.; and Song, W.-L. (2021). Bidirectional planar flexible snake - origami batteries. *Advanced Science*, 8(20), 2101372.
14. Lopez, M.; and Haghshenas-Jaryani, M. (2023). A study of energy-efficient and optimal locomotion in a pneumatic artificial muscle-driven snake robot. *Robotics*, 12(3), 89.
15. Rebolledo, M.; Zeeuwe, D.; Bartz-Beielstein, T.; and Eiben, A.E. (2021). Impact of energy efficiency on the morphology and behaviour of evolved robots. *Proceedings of the GECCO '21: Genetic and Evolutionary Computation Conference Companion*, Lille France, 109-110.

16. Bing, Z.; Lemke, C.; Cheng, L.; Huang, K.; and Knoll, A. (2020). Energy-efficient and damage-recovery slithering gait design for a snake-like robot based on reinforcement learning and inverse reinforcement learning. *Neural Networks*, 129, 323-333.
17. Liu, Y.; and Farimani, A.B. (2021). An energy-saving snake locomotion gait policy obtained using deep reinforcement learning. *arXiv preprint*.
18. Singh, A.; Chiu, W.-Y.; Manoharan, S.H.; and Romanov, A.M. (2022). Energy-efficient gait optimization of snake-like modular robots by using multiobjective reinforcement learning and a fuzzy inference system. *IEEE Access*, 10, 86624-86635.
19. Hannigan, E.; Song, B.; Khandate, G.; Haas-Heger, M.; Yin, J.; and Ciocarlie, M. (2020). Automatic snake gait generation using model predictive control. *Proceedings of the 2020 IEEE International Conference on Robotics and Automation (ICRA)*, Paris, France, 5101-5107.
20. Chen, L.; Ma, S.; Wang, Y.; Li, B.; and Duan, D. (2007). Design and modelling of a snake robot in traveling wave locomotion. *Mechanism and Machine Theory*, 42(12), 1632-1642.
21. Badran, M.; Khan, M.R.; Toha, S.F.; and Abidin, Z.Z. (2021). Multi-objective optimization of snake robot in serpentine locomotion. *IIUM Engineering Journal*, 22(2), 364-383.
22. Pereira, J.L.J.; Oliver, G.A.; Francisco, M.B.; Cunha, S.S.; and Gomes, G.F. (2021). A review of multi-objective optimization: Methods and algorithms in mechanical engineering problems. *Archives of Computational Methods in Engineering*, 29(4), 2285-2308.